

# Resveratrol Inhibits Pathologic Retinal Neovascularization in *Vldlr*<sup>-/-</sup> Mice

Jing Hua,<sup>1,2</sup> Karen I. Guerin,<sup>1,2</sup> Jing Chen,<sup>1</sup> Shaday Michán,<sup>3,4</sup> Andreas Stahl,<sup>1,5</sup> Nathan M. Krah,<sup>1</sup> Molly R. Seaward,<sup>1</sup> Roberta J. Dennison,<sup>1</sup> Aimee M. Juan,<sup>1</sup> Colman J. Hatton,<sup>1</sup> Przemyslaw Sapieha,<sup>1,6</sup> David A. Sinclair,<sup>3</sup> and Lois E. H. Smith<sup>1</sup>

**PURPOSE.** Macular telangiectasia (MacTel) is a vision-threatening retinal disease with unknown pathogenesis and no approved treatment. Very low-density lipoprotein receptor mutant mice (*Vldlr*<sup>-/-</sup>) exhibit critical features of MacTel such as retinal neovascularization and photoreceptor degeneration. In this study, the authors evaluate the therapeutic potential of resveratrol, a plant polyphenol, in *Vldlr*<sup>-/-</sup> mice as a model for MacTel.

**METHODS.** *Vldlr*<sup>-/-</sup> and wild-type mice at postnatal day (P) 21 to P60 or P10 to P30 were treated orally with resveratrol. The number of neovascular lesions was evaluated on retinal flatmounts, and resveratrol effects on endothelial cells were assessed by Western blot for phosphorylated ERK1/2, aortic ring, and migration assays. *Vegf* and *Gfap* expression was evaluated in laser-capture microdissected retinal layers of angiogenic lesions and nonlesion areas from *Vldlr*<sup>-/-</sup> and wild-type retinas.

**RESULTS.** From P15 onward, *Vldlr*<sup>-/-</sup> retinas develop vascular lesions associated with the local upregulation of *Vegf* in photoreceptors and *Gfap* in the inner retina. Oral resveratrol re-

duces lesion formation when administered either before or after disease onset. The reduction of vascular lesions in resveratrol-treated *Vldlr*<sup>-/-</sup> mice is associated with the suppression of retinal *Vegf* transcription. Resveratrol also reduces endothelial ERK1/2 signaling as well as the migration and proliferation of endothelial cells. Furthermore, a trend toward increased *rhodopsin* mRNA in *Vldlr*<sup>-/-</sup> retinas is observed.

**CONCLUSIONS.** Oral administration of resveratrol is protective against retinal neovascular lesions in *Vldlr*<sup>-/-</sup> mice by inhibiting *Vegf* expression and angiogenic activation of retinal endothelial cells. These results suggest that resveratrol might be a safe and effective intervention for treating patients with MacTel. (*Invest Ophthalmol Vis Sci.* 2011;52:2809–2816) DOI: 10.1167/iov.10-6496

Abnormal retinal angiogenesis and choroidal angiogenesis are common causes of vision loss.<sup>1</sup> Macular telangiectasia (MacTel), also known as idiopathic parafoveal telangiectasia, is a retinal neovascular disease in which there is abnormal retinal neovascular proliferation in the perimacular area<sup>2–4</sup> associated with photoreceptor degeneration.<sup>1,4</sup> The pathogenesis of MacTel is not yet understood, though aging might be a contributing factor because MacTel is typically diagnosed in patients in their 50s or 60s. Regrettably, there is no recognized treatment for MacTel to date. Preclinical studies using animal models that mimic MacTel would significantly help to evaluate novel potential therapeutic strategies.

Similar to MacTel and retinal angiomatous proliferation (RAP),<sup>5,6</sup> the very low-density lipoprotein receptor (*VLDLR*) mutant mouse (*Vldlr*<sup>-/-</sup>) shows patchy retinal neovascularization (NV) arising from the deep retinal vascular layer. These changes become visible by the end of the second postnatal week, and by 4 weeks of age the NV lesions extend through the normally avascular photoreceptor layer toward the surface of the retinal pigment epithelium (RPE). NV lesions form subretinal clusters of abnormal microvessels reminiscent of those observed in patients with MacTel.<sup>6,7</sup> *Vegf*-A (*Vegf*) is elevated in *Vldlr*<sup>-/-</sup> retinas and is likely one of the primary causes of the proliferation of subretinal neovascular lesions and their leakiness.<sup>6,8</sup> *Vldlr*<sup>-/-</sup> mouse retinas also show photoreceptor degeneration and Müller glial activation<sup>9</sup> associated with subretinal neovascular lesions, indicating a focal increase of retinal neuronal stress. Importantly, the NV lesions in both MacTel patients and *Vldlr*<sup>-/-</sup> mice originate from the retinal vessels without initial RPE damage, in contrast to wet age-related macular degeneration, in which NV grows from the choroid through defects in Bruch's membrane into the subretinal space.<sup>6</sup> Although the molecular mechanisms leading to these vascular and neuronal lesions in *Vldlr*<sup>-/-</sup> mice are not fully understood, hypoxia, inflammation,<sup>9</sup> and Wnt signaling<sup>10</sup> may play a role in NV development. Antioxidants ameliorate both the retinal degeneration and the vascular pathology in *Vldlr*<sup>-/-</sup> retinas.<sup>6</sup>

From the <sup>1</sup>Department of Ophthalmology, Harvard Medical School, Children's Hospital, Boston, Massachusetts; <sup>2</sup>Department of Pathology, Paul F. Glenn Laboratories for the Biological Mechanisms of Aging, Harvard Medical School, Boston, Massachusetts; <sup>3</sup>Instituto de Geriatria, Institutos Nacionales de Salud, Mexico D.F., Mexico; <sup>4</sup>University Eye Hospital Freiburg, Freiburg, Germany; and <sup>5</sup>Department of Ophthalmology, Maisonneuve-Rosemont Hospital Research Centre, University of Montreal, Montreal, Quebec, Canada.

<sup>2</sup>These authors contributed equally to the work presented here and should therefore be regarded as equivalent authors.

Supported by the Lowy Medical Foundation (MacTel), National Institutes of Health (Grants EY017017 and EY017017-S1), V. Kann Rasmussen Foundation, Roche Foundation for Anemia Research, CHB Mental Retardation and Developmental Disabilities Research Center, RPB Senior Investigator Award, Alcon Research Institute Award (LEHS), Juvenile Diabetes Research Foundation International (JDRF), Knights Templar Eye Foundation, Children's Hospital Boston Manton Center for Orphan Disease (JC), Deutsche Forschungsgemeinschaft (AS), Canadian Institutes of Health Research, Canadian National Institute for the Blind, and Charles A. King Trust Award (PS). DAS supported by grants from the National Institutes of Health (AG028730 and AG027916), Juvenile Diabetes Research Foundation, The Glenn Foundation for Medical Research, and an Ellison Medical Foundation Senior Scholar award.

Submitted for publication August 30, 2010; revised November 10, 2010; accepted December 3, 2010.

Disclosure: J. Hua, None; K.I. Guerin, None; J. Chen, None; S. Michán, None; A. Stahl, None; N.M. Krah, None; M.R. Seaward, None; R.J. Dennison, None; A.M. Juan, None; C.J. Hatton, None; P. Sapieha, None; D.A. Sinclair, None; L.E.H. Smith, None

Corresponding author: Lois E. H. Smith, Harvard Medical School, Children's Hospital Boston, 300 Longwood Avenue, Boston, MA 02115; lois.smith@childrens.harvard.edu.

In this study we evaluated the therapeutic potential of resveratrol, a plant polyphenol, for the treatment of subretinal NV using *Vldlr*<sup>-/-</sup> mice as a model for MacTel. Resveratrol is found in grapes, peanuts, pines, and red wines, and its intake has been associated with a reduced risk of cardiovascular disease.<sup>11</sup> In animal models, resveratrol also inhibits angiogenesis in cancer,<sup>12,13</sup> in development and wound healing through downregulation of the MAPK pathway in endothelial cells, leading to reduced endothelial proliferation and migration.<sup>14</sup> Yet in other conditions such as stroke, myocardial infarction, and ischemia-reperfusion injuries, resveratrol can be proangiogenic while at the same time exerting neuroprotective properties.<sup>15–17</sup>

Our results show that the oral administration of resveratrol significantly suppresses pathologic NV formation in *Vldlr*<sup>-/-</sup> mice when treated after the onset of neovascular lesions but also when started before the lesions fully form. The antiangiogenic and antimigratory effects of resveratrol are seen in an ex vivo aortic ring assay and in cell culture experiments. Additionally, resveratrol treatment significantly reduces *Vegf* transcription in *Vldlr*<sup>-/-</sup> retinas and diminishes VEGF-induced phosphorylation of MAPK in vitro. Together these results suggest resveratrol reduces neovascular lesions in *Vldlr*<sup>-/-</sup> retinas through the downregulation of VEGF and an attenuated response of retinal endothelial cells to angiogenic stimulation.

## METHODS

### Animals and Housing

All studies adhered to the ARVO Statement for the Use of Animals in Ophthalmic and Vision Research and were approved by the Children's Hospital Boston Animal Care and Use Committee. Breeding pairs of mice with insertion mutation of the *Vldlr* gene (B6;129S7-*Vldlr*<sup>tm1Her/J</sup>; stock number 002529) and wild-type (WT) mice on the same genetic background were purchased from the Jackson Laboratory (Bar Harbor, ME). The *Vldlr*<sup>tm1Her</sup> mutation contains a partial deletion of exon 5 in the *Vldlr* gene and an inserted neomycin cassette that disrupts the reading frame; therefore, no *Vldlr* protein is detectable by immunoblot analysis.<sup>18</sup> The homozygous mutant mice are viable and fertile. All animals were housed in a 12-hour light/12-hour dark cycle and given food ad libitum.

### Resveratrol Treatment

Mice were treated with resveratrol using two different protocols. For the first one, weaned (P21) *Vldlr*<sup>-/-</sup> mouse pups were supplied with a defined rodent diet AIN-93G supplemented with 2.4 g resveratrol/kg solid chow (equals 0.36 g/kg body weight, calculated from 150 g/kg body weight daily food intake of a mouse) or control AIN-93G feed<sup>19</sup> (Research Diets Incorporated, New Brunswick, NJ). Fresh food was provided every week until the end of the experiment at P60. In a second experiment, 1 g/kg body weight of a micronized formulation of resveratrol (1 g micronized resveratrol/kg body weight in 10  $\mu$ L of 2% HPMC, 0.2% DOSS, 1% sucrose in water) or vehicle only as control was given by oral gavage to *Vldlr*<sup>-/-</sup> pups daily<sup>20</sup> from postnatal day (P) 10 to P30, before the onset of subretinal neovascularization. Littermate controls were used in all experiments.

### Quantification of Retinal Neovascularization

*Vldlr*<sup>-/-</sup> and control mice were euthanatized at P60 (solid chow fed) or P30 (gavage treated) with lethal doses of tribromoethanol (Avertin; Sigma, St. Louis, MO), and eyes were fixed in 4% paraformaldehyde (PFA) for 1 hour then rinsed in PBS. Retinas were dissected and stained overnight at room temperature with Alexa Fluor 594-conjugated *Griffonia bandeiraea simplicifolia* isolectin B<sub>4</sub> (IB4 Alexa Fluor 594, 1:100 dilution; Molecular Probes, Eugene, OR) in 1 mM CaCl<sub>2</sub> in 1× PBS. Retinas were then washed in 1× PBS for 2 hours and whole-mounted onto Superfrost/Plus microscope slides (Fisher Scientific,

Pittsburgh, PA) with the photoreceptor side down and were mounted in reagent (SlowFade Antifade; Invitrogen, Carlsbad, CA). Images of each of the retinal quadrants were obtained at 5× magnification on a microscope (Z1 AxioObserver; Zeiss, Oberkochen, Germany) with a monochrome digital camera (AxioCam MRm; Zeiss) using the automated merge function (mosaiX; Zeiss) and compatible software (Axio-Vision 4.6.3.0; Zeiss). Subretinal NV lesions were quantified with image editing software (Photoshop; Adobe, Mountain View, CA) in a blinded fashion. Each retina was analyzed at high magnification, and individual NV lesions were outlined using the Lasso tool. The total number of subretinal NV fronds next to the RPE per retina was counted (Supplementary Fig. S1, <http://www.iovs.org/lookup/suppl/doi:10.1167/iovs.10-6496/-DCSupplemental>), and compared between the treated retinas and controls.

### Immunofluorescence of Cryosections

Eyes from *Vldlr*<sup>-/-</sup> and WT mice at P15, P30, and P60 were collected and fixed in 4% PFA for 1 hour at 4°C. The cornea and lens were removed, and the eyecup was immersed in 30% sucrose for 2 hours, embedded in optimum cutting temperature (OCT) medium, and stored at -80°C until processed. Eight-micrometer sections were cut and incubated with IB<sub>4</sub> or primary anti-GFAP antibody (1:1000, Abcam) for 1 hour. After a wash and incubation in the secondary antibody, sections were embedded in reagent (SlowFade Antifade; Invitrogen) with DAPI for microscopy.

### Aortic Ring Assay

Aortic ring assays were carried out as previously described.<sup>21,22</sup> In brief, adult *Vldlr*<sup>-/-</sup> and WT mice were perfused with PBS after a lethal intraperitoneal dose of tribromoethanol (Avertin; Sigma). Aortas were dissected free from adventitia and cut into 1-mm-thick rings. Individual rings were placed in growth factor-reduced basement membrane matrix (Matrigel; BD Biosciences, Franklin Lakes, NJ) in 24-well tissue culture plates and incubated for 4 days in medium (EBM-2; Clonetics, Walkersville, MD) containing growth factor boost but no steroids (CC-4176; Clonetics).<sup>23</sup> Resveratrol (50  $\mu$ M) or vehicle solution (2% HPMC, 0.2% DOSS in water) was added to the indicated wells. Microphotographs of each well were taken after 6 days' incubation, and images were quantified (Photoshop; Adobe) by measuring the area covered by outgrowth of the aortic ring. Results are expressed as mean  $\pm$  SEM.

### Laser-Capture Microdissection of Retinal Layers

Laser-capture microdissection of distinct retinal regions in cross-section was carried out as previously described.<sup>24</sup> Eyes of P30 *Vldlr*<sup>-/-</sup> and control WT mice were embedded in OCT compound, and 8- $\mu$ m sections were mounted onto RNase-free polyethylene-naphtholate glass slides (PEN-membrane slides; Leica Microsystems, Wetzlar, Germany) and immediately stored at -80°C. Slides containing frozen sections were fixed with 75% ethanol for 15 seconds, stained with fluoresceinated isolectin B<sub>4</sub> (Alexa Fluor 594 [Molecular Probes], 1:50 dilution in 1 mM CaCl<sub>2</sub> in PBS), and dehydrated in 70% and 95% ethanol. Layers within and outside the NV lesions, or corresponding layers in WT eyes, were laser microdissected (LMD 6000 system; Leica Microsystems) and collected directly into RLT lysis buffer. Material from each cell layer from an individual eye was kept separately, and RNA was isolated (RNeasy MicroKit; Qiagen, Valencia, CA).

### Quantitative Analysis of Gene Expression

RNA samples from whole retina or laser-captured samples were treated with DNase I (Qiagen) and then reverse transcribed (Invitrogen) to cDNA for quantitative real-time PCR (qRT-PCR). PCR primers targeting murine *Vegf* and *Gfap* and an internal control gene, *cyclophilin*, were designed using NCBI Primer Blast with sequences that specifically detect all known isoforms of the target genes. Gene expression was quantified with a sequence detection system (7700 TaqMan; ABI Prism) and the SYBR Green master mix kit. Data were analyzed using the  $\Delta\Delta$ -Ct method.

## Boyden Chamber Cell Migration Assay

Human renal microvascular endothelial cells (HRMECs; Cell Systems) at approximately 70% confluence were serum starved overnight and seeded on Boyden Chambers (25,000 cells/well). Cells were incubated in basal media with 0.5% FBS and 20 ng/mL VEGF or bFGF and 50  $\mu$ M resveratrol or vehicle. After 4 hours at 37°C and 5% CO<sub>2</sub>, the cells were fixed in 4% PFA and stained with DAPI. The cleaned membrane was embedded for microscopy, and migrated cells were quantified.

## HRMEC Culture and Conditional Stimulation

HRMECs were cultured in six-well plates until they were approximately 70% confluent, then they were serum starved overnight. The cells were incubated for 4 hours with resveratrol or vehicle at 37°C and 5% CO<sub>2</sub>; 10 ng/mL VEGF (VEGF<sub>165</sub>) was then added, and cells were incubated for 15 minutes, washed twice in 4°C PBS, and lysed in RIPA buffer with phosphatase and protease inhibitors (Sigma). Samples were centrifuged at 4°C, and supernatant protein samples were collected for Western blots.

## Western Blot Analysis

Protein extracts of lysates from HRMEC cultures or from homogenized retinas of *Vldlr*<sup>-/-</sup> mice were used in Western blots. Total protein concentration was measured using a BCA assay (Pierce, Rockford, IL). Fifty micrograms of each protein sample was loaded on an SDS-PAGE gel for electrophoresis. The gel was blotted onto a polyvinylidene difluoride membrane. The primary antibodies were rabbit monoclonal against total ERK1/2, p42/44 phosphorylated ERK1/2 (4695 and 43965, respectively; Cell Signaling Technology, Danvers, MA), and rabbit polyclonal anti-Fgf2 (R&D Systems). The primary antibody was applied overnight in 5% BSA at 4°C. Membranes were then incubated with horseradish peroxidase-conjugated goat antibody to rabbit IgG (1:1000, Amersham) and developed on Kodak film. Antibodies were used according to manufacturer's recommendations. Samples from three independent experiments for each condition were used in the Western blot. Densitometry was analyzed using ImageJ software (developed by Wayne Rasband, National Institutes of Health, Bethesda, MD; available at <http://rsb.info.nih.gov/ij/index.html>).

## Statistical Analysis

All values are expressed as mean  $\pm$  SEM. Comparison between two groups was analyzed using Student's *t*-test. Comparison between more than two groups was performed using ANOVA with Tukey-Kramer HSD correcting for multiple testing. Differences between experimental groups were considered statistically significant or highly significant at values of  $P \leq 0.05$  or  $P \leq 0.01$ , respectively.

## RESULTS

### Characterization of Retinal Neovascularization in *Vldlr*<sup>-/-</sup> Mice

NV in *Vldlr*<sup>-/-</sup> mice is first detectable in the outer nuclear layer (ONL) at P15 and is associated with Müller cell activation and local neuronal cell death.<sup>6</sup> We confirmed these characteristic findings in *Vldlr*<sup>-/-</sup> retinas with deep penetrating retinal vessels originating from the vasculature in the outer plexiform layer (OPL) of the retina, growing through the normally avascular ONL into the subretinal space at P15 (Fig. 1A). We also confirmed focal activation of Müller cells in the *Vldlr*<sup>-/-</sup> retinas associated with the sites of vascular lesion (Fig. 1B). In addition, 3D reconstruction of the neovascular lesions in P30 *Vldlr*<sup>-/-</sup> mice demonstrates that the abnormal vessels in the ONL are connected to the deep layer of the retinal capillary network in the OPL and extend downward to form abnormal neovascular clusters on the surface of the RPE, demonstrating the retinal origin of these subretinal vascular clusters (Figs. 1C, 1D).

### Inhibition of Retinal Neovascularization in *Vldlr*<sup>-/-</sup> Mice Treated with Resveratrol

To evaluate the potential therapeutic effect of resveratrol after the onset of subretinal NV, *Vldlr*<sup>-/-</sup> mice and littermate controls were fed with regular or resveratrol-supplemented (0.36 g/kg/d) solid chow from P21 through P60. Retinas from *Vldlr*<sup>-/-</sup> mice treated with resveratrol showed significantly fewer subretinal NV lesions at P60 ( $102.1 \pm 4.9$  lesions per

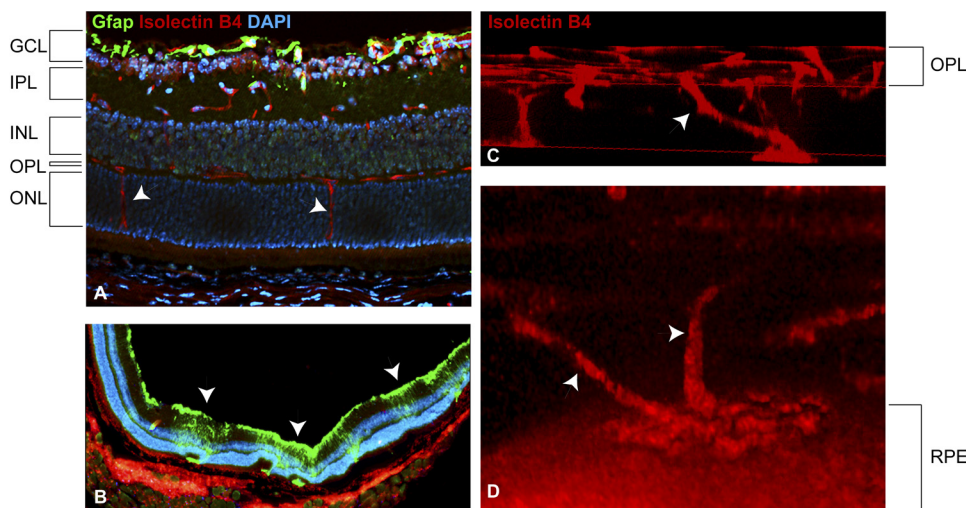


**FIGURE 1.** Pathologic subretinal neovascularization in *Vldlr*<sup>-/-</sup> mouse retina. (A) Cross-section of *Vldlr*<sup>-/-</sup> retina at P15. Endothelial cells stained with isolectin B4 (red) at the early stage of abnormal growth of deeper penetrating vessels (white arrows) extending from the OPL, where the deep layer of retinal capillary networks normally stop, across the ONL toward the photoreceptor outer segments and RPE. Gfap was present (green) in the astrocytes around the superficial layer of vessels only. (B) At P30, multiple foci of positive GFAP staining (green) were present in Müller cells spanning the retinal layers (white arrows). (C, D) 3D reconstruction of isolectin B4 stained neovascularization between the OPL and RPE layers at P30, culminating in a subretinal neovascular mass on the surface of the photoreceptor side of the RPE (white arrows).



retina;  $n = 18$ ) compared with controls ( $166.7 \pm 11.9$  lesions per retina;  $n = 15$ ;  $P < 0.00001$ ; Fig. 2A). To investigate whether resveratrol also prevents the early stages of NV formation, we treated *Vldlr*<sup>-/-</sup> mice from P10 to P30 with resveratrol (1 g/kg/d by oral gavage). In this approach, resveratrol treatment coincides with the onset of NV formation (P15). We found that resveratrol reduced the number of subretinal NV lesions ( $22.6 \pm 5.4$  vs.  $70.9 \pm 10.2$  lesions per retina;  $n \geq 10$ ;  $P = 0.0001$ ; Fig. 2B).

### Resveratrol Inhibits Vascular Sprouting Ex Vivo

To confirm the antiangiogenic effect of resveratrol in vitro, we used aortic explants isolated from WT and *Vldlr*<sup>-/-</sup> mice. Resveratrol treatment reduced the area of endothelial cell sprouting in both WT and *Vldlr*<sup>-/-</sup> aortas (WT,  $9.7 \pm 0.6$  mm<sup>2</sup> vs.  $21.8 \pm 0.1$  mm<sup>2</sup>,  $n = 6$  per group,  $P = 3.7 \times 10^{-8}$ ; *Vldlr*<sup>-/-</sup>,  $13.0 \pm 1.0$  mm<sup>2</sup> vs.  $24.3 \pm 2.3$  mm<sup>2</sup>,  $n = 6$  per group,  $P < 0.002$ ; Fig. 2C). This suggests that the antiangiogenic effect of resveratrol is not dependent on the *Vldlr* mutation.

### Neovascular Lesions in the *Vldlr*<sup>-/-</sup> Retina Show Focal Upregulation of *Vegf* and *Gfap*

Previous studies have shown an upregulation of *Vegf* and *Gfap* in the whole retina of *Vldlr*<sup>-/-</sup> mice compared with WT controls.<sup>6,8</sup> To quantify *Vegf* and *Gfap* gene expression specifically in the lesions, we used laser capture microdissection to isolate individual retinal layers in lesion areas and in nonlesion areas in *Vldlr*<sup>-/-</sup> retinas and in the corresponding layers of WT control retinas. Four layers were captured in each group: ganglion cell layer (GCL), inner nuclear layer (INL), outer nuclear layer (ONL) and RPE layer (Fig. 3A). We used quantitative RT-PCR on each laser captured retinal layer to assess the mRNA expression of *Vegf* and *Gfap*.

We find the highest expression of *Vegf* mRNA in ONL and RPE of *Vldlr*<sup>-/-</sup> around the area of the NV lesions. *Vegf* mRNA from the *Vldlr*<sup>-/-</sup> ONL lesion area was increased 6.7-fold compared with the ONL of an adjacent nonlesion region in the *Vldlr*<sup>-/-</sup> retina and increased 18.6-fold over ONL in WT reti-

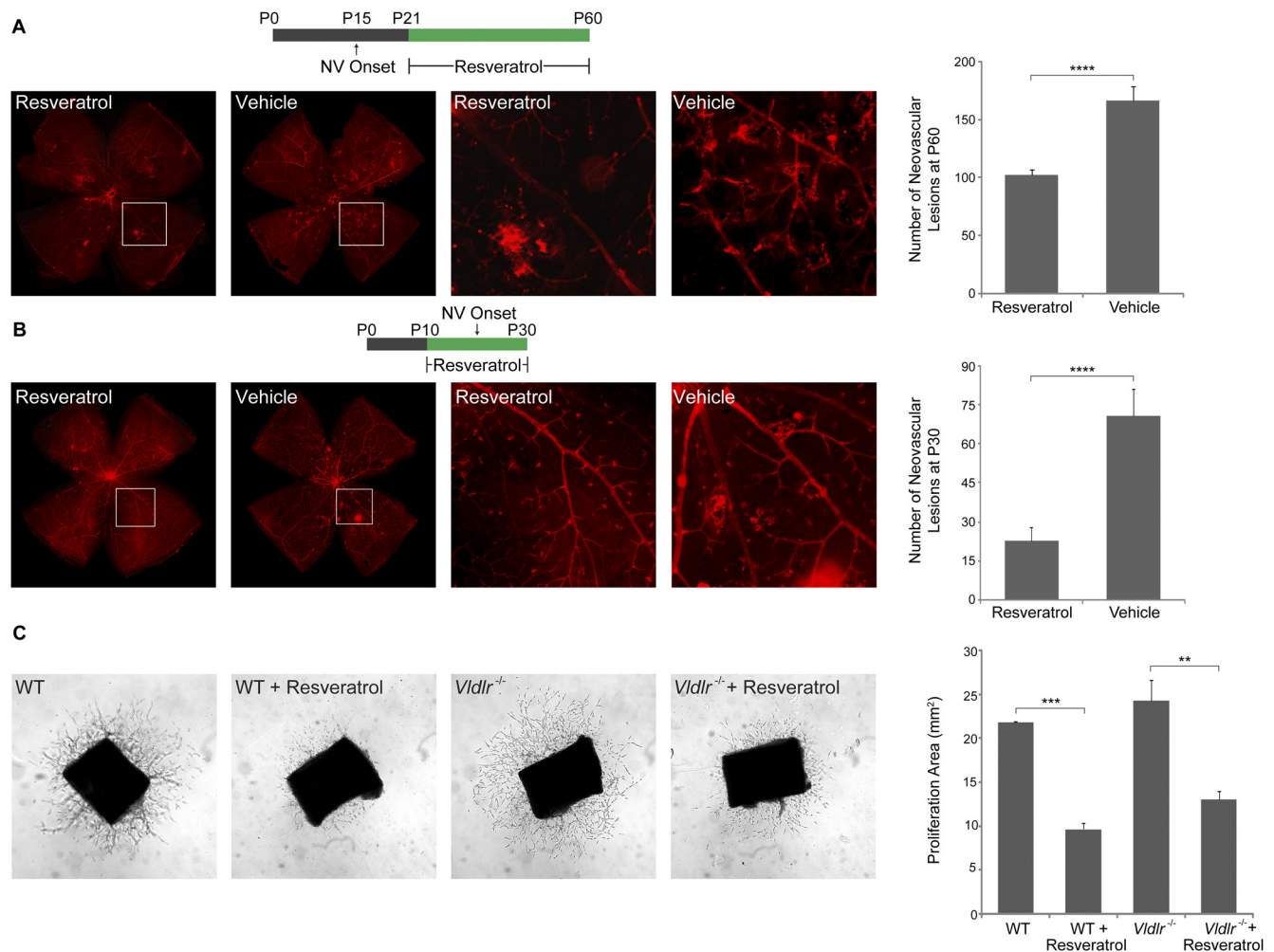


**FIGURE 2.** Resveratrol inhibited pathologic subretinal neovessels in *Vldlr*<sup>-/-</sup> mice. (A) Retinal whole mounts from resveratrol-treated (P21–P60) and control *Vldlr*<sup>-/-</sup> mice showing retinal vessels stained with isolectin B4 at P60. Pathologic subretinal neovascularization is shown in red. Indicated areas with NV in the subretinal space are shown with higher magnification. Numbers of subretinal lesions were quantified and graphed (Student's *t*-test,  $n = 18$  and  $n = 15$ , respectively; \*\*\*\* $P \leq 0.0001$ ). Resveratrol treatment from P21 to P60 significantly reduced subretinal NV in *Vldlr*<sup>-/-</sup> mice compared with the control group. (B) Retinal whole mount of P30 *Vldlr*<sup>-/-</sup> mice treated with resveratrol before NV onset (P10–P30) shows significantly less NV than vehicle treatment. Quantified lesions are shown in the bar graph (Student's *t*-test,  $n = 16$  and  $n = 10$ , respectively; \*\*\*\* $P \leq 0.0001$ ). (C) Aortic ring assay. Representative photomicrographs of aortic ring sections from 6-week-old *Vldlr*<sup>-/-</sup> and WT mice cultured in basement membrane matrix and treated with resveratrol. Resveratrol treatment significantly reduced endothelial sprouting of aortic rings isolated from both WT and *Vldlr*<sup>-/-</sup> mice compared with vehicle treatment group (\*\*\* $P \leq 0.001$  in WT, \*\* $P = 0.002$  in *Vldlr*<sup>-/-</sup>;  $n = 6$  for each group).

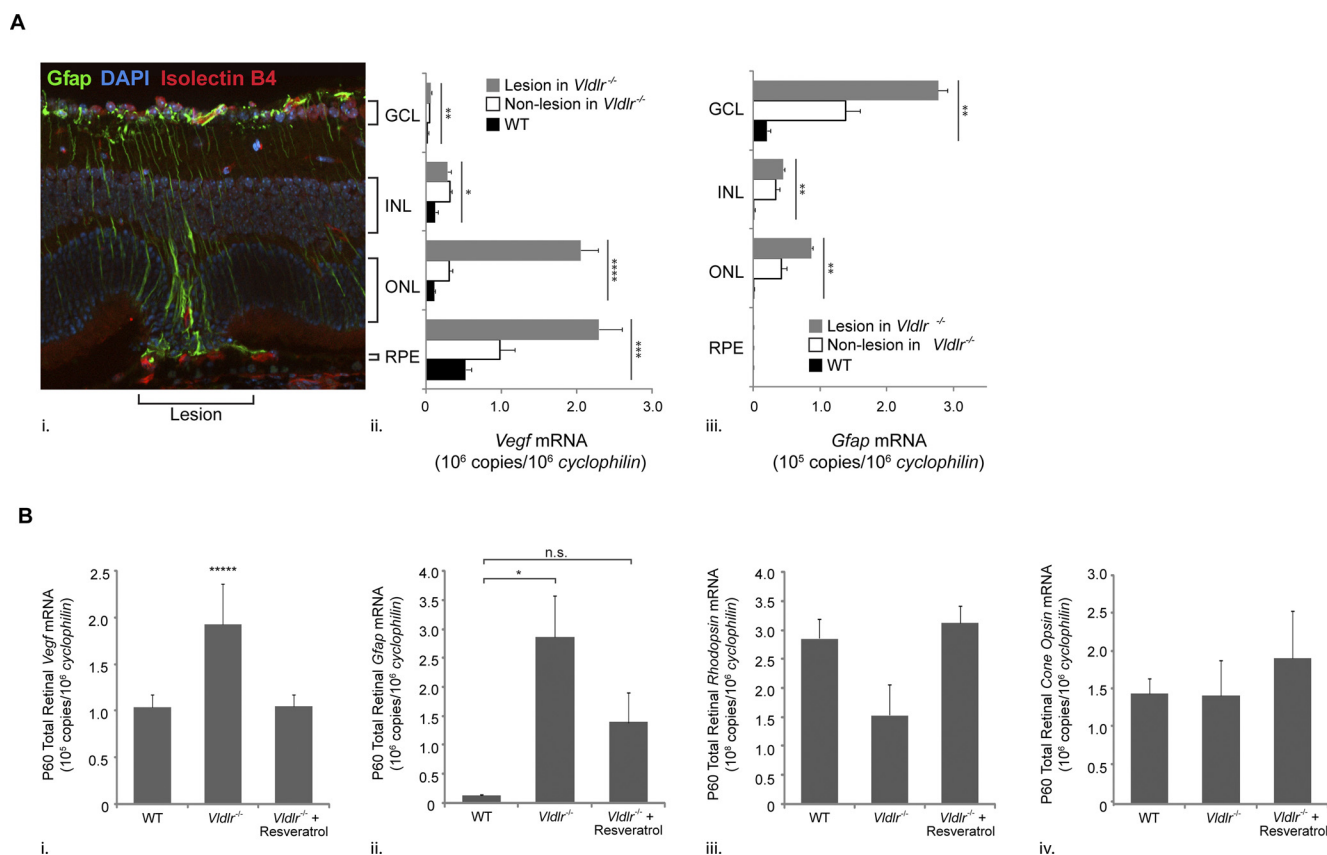


**FIGURE 3.** (A) Focal upregulation of *Vegf* and *Gfap* mRNA in neurovascular lesions of *Vldlr*<sup>-/-</sup> mice. (Ai) Cross-section of the *Vldlr*<sup>-/-</sup> retina at P30 shows focalized activation of Müller cells with positive GFAP staining in and above the neovascular lesion. (Aii) Analysis of VEGF mRNA expression in laser-capture microdissected samples with qRT-PCR. *Vegf* mRNA was upregulated most in the ONL in the lesion and also in the RPE compared with WT. (Aiii) *Gfap* transcription was upregulated throughout the layers of lesion, particularly in the ONL. ANOVA test was positive in both (Aii) and (Aiii). Tukey Kramer ( $\alpha = 0.05$ –0.00001) was applied for mean comparisons in each location and target gene (*Vegf* or *Gfap*). Asterisks indicate the significant difference from other samples within the group ( $\alpha = *0.05$ , \*\*0.01, \*\*\*0.001, \*\*\*\*0.0001, and \*\*\*\*\*0.00001). (B) Resveratrol treatment reduced *Vegf* and *Gfap* transcription in *Vldlr*<sup>-/-</sup> total retinas at P60. (Bi) The amount of *Vegf* mRNA in *Vldlr*<sup>-/-</sup> retinas was significantly different from both WT retinas and *Vldlr*<sup>-/-</sup> retinas treated with resveratrol from P21 to P60 (positive ANOVA; Tukey Kramer \*\*\*\* $\alpha = 0.00001$ ;  $n = 3$  for each group). (Bii) *Gfap* mRNA was significantly upregulated in *Vldlr*<sup>-/-</sup> mice (positive ANOVA; Tukey Kramer \* $\alpha = 0.05$ ;  $n = 3$  for each group), and resveratrol decreased the amount of transcript. (Biii) A trend of preserved *Rhodopsin* mRNA expression was detected in resveratrol-treated *Vldlr*<sup>-/-</sup>. (Biv) No difference was found in *Cone Opsin* expression.

nas. The RPE layer directly below the lesions in *Vldlr*<sup>-/-</sup> retinas also had significantly elevated expression of *Vegf* mRNA, with a 2.4-fold increase compared with the nonlesion region and a 4.4-fold increase relative to RPE of WT eyes. *Vegf* mRNA levels in the GCL and INL of NV lesions from *Vldlr*<sup>-/-</sup> retinas were also higher than in the WT layers (2.4- and 2.3-fold increases, respectively) but did not differ from the adjacent nonlesion regions in these *Vldlr*<sup>-/-</sup> layers (Fig. 3A). These data suggest that the main source of retinal *Vegf* upregulation in *Vldlr*<sup>-/-</sup> retinas is from the ONL and RPE in the lesion sites.

NV lesions in *Vldlr*<sup>-/-</sup> retinas also have the highest upregulation of *Gfap* mRNA, which suggests increased local retinal stress (Fig. 3A). *Gfap* mRNA expression levels in GCL and INL in lesion sites are greatly increased compared with the corresponding layers in WT retinas, with 13.8- and 24.2-fold increases, respectively. *Gfap* mRNA expression was 68.0-fold greater in *Vldlr*<sup>-/-</sup> NV lesions than in ONL and twofold greater than nonlesion ONL in *Vldlr*<sup>-/-</sup> mice ANOVA ( $\alpha = 0.001$ ;  $n = 4$ ).

### Resveratrol Treatment Reduces Vegf and Gfap Expression in *Vldlr*<sup>-/-</sup> Retinas

As expected, based on layer-specific analysis, the *Vegf* mRNA levels in whole retinas from *Vldlr*<sup>-/-</sup> mice were significantly

higher than in WT retinas (Fig. 3Bi). Interestingly, resveratrol treatment from P21 to P60 in *Vldlr*<sup>-/-</sup> mice markedly reduced *Vegf* mRNA expression to levels found in WT retinas ANOVA ( $\alpha = 0.0001$ ;  $n = 3$  per group). *Gfap* mRNA expression in *Vldlr*<sup>-/-</sup> retinas was also significantly higher than in WT retinas (Fig. 3Bii), and resveratrol treatment reduced the transcript level close to twofold. These results suggest that resveratrol treatment in *Vldlr*<sup>-/-</sup> retinas was associated with a decrease in retinal *Vegf* expression and a reduction of local glial stress. In addition, *Rhodopsin* mRNA level in the *Vldlr*<sup>-/-</sup> retinas showed a trend toward a decrease compared with WT, indicating that potential rod photoreceptor loss may be associated with the *Vldlr*<sup>-/-</sup> phenotype (Fig. 3Biii). Levels of *Cone opsin* mRNA did not vary significantly between WT and *Vldlr*<sup>-/-</sup> retinas, possibly reflecting primary damage to rods but not to cones (Fig. 3Biv).

### Resveratrol Inhibits Endothelial Cell Migration and ERK1/2 Phosphorylation

We next examined the effects of resveratrol on downstream signaling. An in vitro migration assay with HRMECs demonstrated that VEGF-stimulated migration of HRMEC is significantly inhibited by resveratrol ( $147 \pm 2$  cells/membrane in

VEGF incubated wells vs.  $26 \pm 4$  cells/membrane with VEGF and resveratrol;  $P = 6.0 \times 10^{-6}$ ;  $n = 3$  per group; Fig. 4A). This antimigratory effect of resveratrol is not VEGF specific because we observed a similar inhibition of bFGF-induced HRMEC migration ( $289 \pm 12$  cells/membrane in bFGF-incubated wells and  $88 \pm 12$  cells/membrane in wells incubated with both bFGF and resveratrol;  $P = 0.0001$ ;  $n = 3$  per group; Supplementary Fig. S2A, <http://www.iovs.org/lookup/suppl/doi:10.1167/iovs.10-6496/-DCSupplemental>). Resveratrol treatment also reduced retinal expression of Fgf2 protein, the murine form of basic FGF (bFGF; Supplementary Fig. S2B, <http://www.iovs.org/lookup/suppl/doi:10.1167/iovs.10-6496/-DCSupplemental>), supporting the notion that resveratrol effects are not exclusively limited to antagonizing VEGF.

Given that the ERK1/2 MAPK pathways are important for mediating VEGF-induced endothelial migration and proliferation,<sup>25</sup> we evaluated the effect of resveratrol on VEGF-induced ERK1/2 phosphorylation in HRMECs. We found that resveratrol-treated HRMECs have significantly less phosphorylated ERK1/2 than control ( $22\% \pm 3\%$  of total ERK1/2 with basal media,  $51\% \pm 5\%$  with VEGF, and  $11\% \pm 7\%$  with VEGF + resveratrol; Student's *t*-test between the latter two groups;  $P < 0.001$ ;  $n = 3$ ; Figs. 4B, 4C). These findings suggest that the effect of resveratrol on VEGF-induced endothelial migration is likely mediated, at least in part, through a decreased activation state of ERK1/2.

## DISCUSSION

There is no clinically recognized treatment for MacTel to date. Several recent small-scale studies find that intravitreal injection of bevacizumab reduces vascular leakage in MacTel patients. However, the effects of bevacizumab on photoreceptor cell loss or improvement of visual acuity in MacTel patients are less clear.<sup>26–28</sup> Similarly, other small-scale studies on RAP, with retinal NV like MacTel, find that intraocular injection of VEGF-inhibitors reduce vascular leakage in the short term (up to 22 months).<sup>29–33</sup> However, there are no data for the long-term outcome of these treatments, especially with regard to visual acuity. This is important in light of studies reporting that direct inhibition of VEGF may decrease neuroprotection,<sup>34</sup> which might have negative consequences in an already stressed retina. Our study finds that oral treatment with resveratrol re-

duces NV in *Vldlr*<sup>−/−</sup> mice and may be a novel potential therapeutic option for MacTel patients.

The *Vldlr*<sup>−/−</sup> mouse model replicates several critical features of MacTel and RAP, such as NV proliferation originating from retinal vessels with focal leakage and photoreceptor cell death. Increased VEGF expression is suggested by the vascular leakage in MacTel<sup>26</sup> and RAP,<sup>29</sup> and this notion is supported by the reduction of NV progression with bevacizumab or ranibizumab (Lucentis) injections in these patients. Concordant with these clinical observations, the upregulation of *Vegf* in *Vldlr*<sup>−/−</sup> retinas is found in this study and several previous reports.<sup>6–8</sup> In addition, our investigation is the first to describe a distinct localized expression pattern of *Vegf* and *Gfap* in *Vldlr*<sup>−/−</sup> retinas. The upregulation of *Vegf* is found to be most prominent in the ONL of neovascular lesion areas. *Gfap* mRNA is also found throughout the *Vldlr*<sup>−/−</sup> eyes, most abundantly within the NV lesion areas; however, unlike *Vegf*, *Gfap* is found mainly in the GCL (Fig. 3A). Glial cell activation in this model is consistent with reports that Müller glial cells may be involved in MacTel.<sup>35</sup>

Importantly, our results provide evidence that oral resveratrol reduces pathologic NV in *Vldlr*<sup>−/−</sup> mouse retinas when administered either before or after the onset of the formation of NV lesions. Resveratrol may be useful for clinical interventions at different stages of MacTel. We found that the reduction of retinal NV in resveratrol-treated mice is associated with a reduction of retinal *Vegf* transcription in *Vldlr*<sup>−/−</sup> retinas. Moreover, resveratrol also reduces the migration and proliferation of endothelial cells toward different angiogenic cues in both *Vldlr*<sup>−/−</sup> and WT mice in aortic ring explant assays, suggesting that the antiangiogenic effect of resveratrol is not dependent on the *Vldlr* mutation. This observation is in line with a previous report showing that resveratrol regulates pathologic angiogenesis through a novel sirtuin-independent elongation factor 2 kinase pathway.<sup>36</sup> We found that although some inflammation markers, such as *TNFα*, are upregulated in *Vldlr*<sup>−/−</sup> retinas compared with wild-type controls, as reported previously,<sup>9</sup> resveratrol treatment in *Vldlr*<sup>−/−</sup> retinas does not significantly change the overall inflammation profile of these markers compared with nontreated *Vldlr*<sup>−/−</sup> retinas (data not shown), suggesting that the protective effects of resveratrol in this model are not caused primarily by alterations of inflammatory pathways. In addition, resveratrol inhibits bFGF-induced endo-

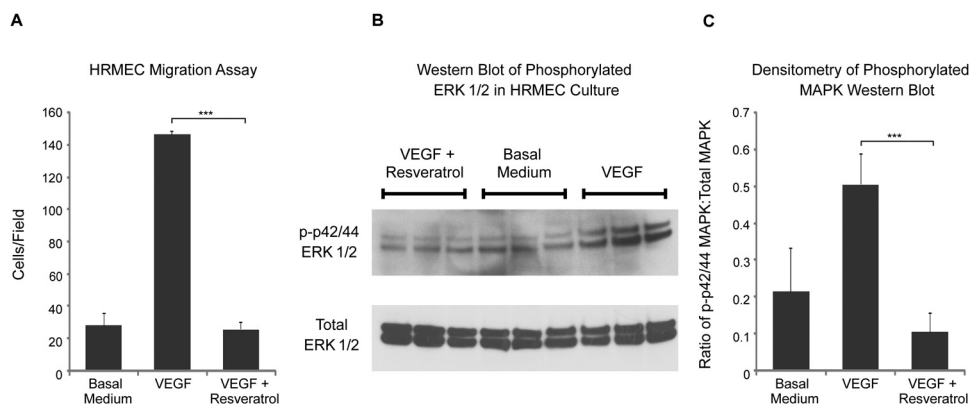


**FIGURE 4.** Reduced HRMEC migration and ERK1/2 phosphorylation with resveratrol treatment. (A) Endothelial cell migration assay in a Boyden chamber. In the presence of VEGF (20 ng/mL), coincubation with resveratrol (50  $\mu$ M) significantly reduced the migration of HRMEC after 4 hours (Student's *t*-test,  $***P \leq 0.0001$ ;  $n = 3$  for each group). (B) Western blot of phosphorylated ERK1/2 and total ERK1/2 in HRMECs. (C) Pretreatment with resveratrol before stimulation with VEGF in HRMEC monolayer culture significantly diminished the p-ERK1/2 to total ERK1/2 ratio, compared with wells without resveratrol. (Student's *t*-test,  $***P \leq 0.001$ ;  $n = 3$  for each group).



thelial cell migration, indicating that the molecular mechanism of resveratrol-induced inhibition of EC sprouting and migration is likely mediated by one or more of the intracellular signaling cascades that are shared by various growth factors. Our data identify the ERK1/2 signaling pathways as one of these shared intracellular signaling pathways. Our results are in line with a previous study demonstrating that resveratrol inhibits bFGF-induced ERK1/2 phosphorylation in bovine aortic endothelial cell culture.<sup>14</sup> Importantly, based on the trend of rescued *Rhodopsin* expression in resveratrol-treated eyes, this compound may also, directly or indirectly, protect against rod photoreceptor degeneration, which agrees with a previous report<sup>6</sup> and supports investigation into the potential benefits of resveratrol in treating patients.

Overall, the significant protective effects of resveratrol observed in *Vldlr*<sup>-/-</sup> mice suggest the possibility of using resveratrol as a safe treatment option for MacTel. We used a daily dose of 0.36 or 1.0 g resveratrol/kg body weight, which is considered feasible for humans.<sup>19</sup> We found that resveratrol at these concentrations inhibits retinal NV formation and is likely to preserve photoreceptors. The effects of resveratrol may not be limited to the pathways investigated in this study because resveratrol has been found to have cytoprotective properties in ischemic conditions such as stroke, myocardial infarction and ischemia-reperfusion injuries<sup>15-17</sup> and can also act as an antioxidant.<sup>37-41</sup> In summary, our study provides the first evidence that the oral administration of resveratrol is a potential, safe, and effective intervention for treating patients with MacTel. These findings may be extended to similar neovascular retinal conditions such as RAP.

## Acknowledgments

The authors thank Peter Elliott and David Gagne (Sirtris Pharmaceuticals) for advice on formulating and delivering resveratrol.

## References

- Klein R, Peto T, Bird A, Vannewkirk MR. The epidemiology of age-related macular degeneration. *Am J Ophthalmol*. 2004;137:486-495.
- Chew E, Gillies M, Bird A. Macular telangiectasia: a simplified classification. *Arch Ophthalmol*. 2006;124:573-574.
- Gass JD. Histopathologic study of presumed parafoveal telangiectasis. *Retina*. 2000;20:226-227.
- Yannuzzi LA, Bardal AM, Freund KB, Chen KJ, Eandi CM, Blodi B. Idiopathic macular telangiectasia. *Arch Ophthalmol*. 2006;124:450-460.
- Heckenlively JR, Hawes NL, Friedlander M, et al. Mouse model of subretinal neovascularization with choroidal anastomosis. *Retina*. 2003;23:518-522.
- Dorrell MI, Aguilar E, Jacobson R, et al. Antioxidant or neurotrophic factor treatment preserves function in a mouse model of neovascularization-associated oxidative stress. *J Clin Invest*. 2009;119:611-623.
- Hu W, Jiang A, Liang J, et al. Expression of VLDLR in the retina and evolution of subretinal neovascularization in the knockout mouse model's retinal angiomatous proliferation. *Invest Ophthalmol Vis Sci*. 2008;49:407-415.
- Li C, Huang Z, Kingsley R, et al. Biochemical alterations in the retinas of very low-density lipoprotein receptor knockout mice: an animal model of retinal angiomatous proliferation. *Arch Ophthalmol*. 2007;125:795-803.
- Chen Y, Hu Y, Moiseyev G, Zhou KK, Chen D, Ma JX. Photoreceptor degeneration and retinal inflammation induced by very low-density lipoprotein receptor deficiency. *Microvasc Res*. 2009;78:119-127.
- Chen Y, Hu Y, Lu K, Flannery JG, Ma JX. Very low density lipoprotein receptor, a negative regulator of the wnt signaling pathway and choroidal neovascularization. *J Biol Chem*. 2007;282:34420-34428.
- Hung LM, Chen JK, Huang SS, Lee RS, Su MJ. Cardioprotective effect of resveratrol, a natural antioxidant derived from grapes. *Cardiovasc Res*. 2000;47:549-555.
- Igura K, Ohta T, Kuroda Y, Kaji K. Resveratrol and quercetin inhibit angiogenesis in vitro. *Cancer Lett*. 2001;171:11-16.
- Tseng SH, Lin SM, Chen JC, et al. Resveratrol suppresses the angiogenesis and tumor growth of gliomas in rats. *Clin Cancer Res*. 2004;10:2190-2202.
- Brakenhielm E, Cao R, Cao Y. Suppression of angiogenesis, tumor growth, and wound healing by resveratrol, a natural compound in red wine and grapes. *FASEB J*. 2001;15:1798-1800.
- Kaga S, Zhan L, Matsumoto M, Maulik N. Resveratrol enhances neovascularization in the infarcted rat myocardium through the induction of thioredoxin-1, heme oxygenase-1 and vascular endothelial growth factor. *J Mol Cell Cardiol*. 2005;39:813-822.
- Dong W, Li N, Gao D, Zhen H, Zhang X, Li F. Resveratrol attenuates ischemic brain damage in the delayed phase after stroke and induces messenger RNA and protein express for angiogenic factors. *J Vasc Surg*. 2008;48:709-714.
- Hsieh YH, Huang SS, Wei FC, Hung LM. Resveratrol attenuates ischemia-reperfusion-induced leukocyte-endothelial cell adhesive interactions and prolongs allograft survival across the MHC barrier. *Circ J*. 2007;71:423-428.
- Frykman PK, Brown MS, Yamamoto T, Goldstein JL, Herz J. Normal plasma lipoproteins and fertility in gene-targeted mice homozygous for a disruption in the gene encoding very low density lipoprotein receptor. *Proc Natl Acad Sci U S A*. 1995;92:8453-8457.
- Baur JA, Pearson KJ, Price NL, et al. Resveratrol improves health and survival of mice on a high-calorie diet. *Nature*. 2006;444:337-342.
- Milne JC, Lambert PD, Schenk S, et al. Small molecule activators of SIRT1 as therapeutics for the treatment of type 2 diabetes. *Nature*. 2007;450:712-716.
- Bellacien K, Lewis EC. Aortic ring assay. *J Vis Exp*. 2009;33:pii:1564.
- Zhu WH, Iurlaro M, MacIntyre A, Fogel E, Nicosia RF. The mouse aorta model: influence of genetic background and aging on bFGF- and VEGF-induced angiogenic sprouting. *Angiogenesis*. 2003;6:193-199.
- Sapieha P, Sirinyan M, Hamel D, et al. The succinate receptor GPR91 in neurons has a major role in retinal angiogenesis. *Nat Med*. 2008;14:1067-1076.
- Lofqvist C, Chen J, Connor KM, et al. IGFBP3 suppresses retinopathy through suppression of oxygen-induced vessel loss and promotion of vascular regrowth. *Proc Natl Acad Sci U S A*. 2007;104:10589-10594.
- LaMontagne KR Jr, Moses MA, Wiederschain D, et al. Inhibition of MAP kinase kinase causes morphological reversion and dissociation between soft agar growth and in vivo tumorigenesis in angiosarcoma cells. *Am J Pathol*. 2000;157:1937-1945.
- Kovach JL, Rosenfeld PJ. Bevacizumab (avastin) therapy for idiopathic macular telangiectasia type II. *Retina*. 2009;29:27-32.
- Gamulescu MA, Walter A, Sachs H, Helbig H. Bevacizumab in the treatment of idiopathic macular telangiectasia. *Graefes Arch Clin Exp Ophthalmol*. 2008;246:1189-1193.
- Charbel Issa P, Finger RP, Holz FG, Scholl HP. Eighteen-month follow-up of intravitreal bevacizumab in type 2 idiopathic macular telangiectasia. *Br J Ophthalmol*. 2008;92:941-945.
- Meyerle CB, Freund KB, Iturralde D, et al. Intravitreal bevacizumab (Avastin) for retinal angiomatous proliferation. *Retina*. 2007;27:451-457.
- Joeres S, Heussen FM, Treziak T, Bopp S, Jousen AM. Bevacizumab (Avastin) treatment in patients with retinal angiomatous proliferation. *Graefes Arch Clin Exp Ophthalmol*. 2007;245:1597-1602.
- Costagliola C, Romano MR, dell'Omo R, Cipollone U, Polisena P. Intravitreal bevacizumab for the treatment of retinal angiomatous proliferation. *Am J Ophthalmol*. 2007;144:449-451.
- Lai TY, Chan WM, Liu DT, Lam DS. Ranibizumab for retinal angiomatous proliferation in neovascular age-related macular degeneration. *Graefes Arch Clin Exp Ophthalmol*. 2007;245:1877-1880.

33. Konstantinidis L, Mameletzi E, Mantel I, Pournaras JA, Zografos L, Ambresin A. Intravitreal ranibizumab (Lucentis) in the treatment of retinal angiomatous proliferation (RAP). *Graefes Arch Clin Exp Ophthalmol*. 2009;247:1165-1171.
34. Nishijima K, Ng YS, Zhong L, et al. Vascular endothelial growth factor-A is a survival factor for retinal neurons and a critical neuroprotectant during the adaptive response to ischemic injury. *Am J Pathol*. 2007;171:53-67.
35. Koizumi H, Slakter JS, Spaide RF. Full-thickness macular hole formation in idiopathic parafoveal telangiectasis. *Retina*. 2007;27:473-476.
36. Khan AA, Dace DS, Ryazanov AG, Kelly J, Apte RS. Resveratrol regulates pathologic angiogenesis by a eukaryotic elongation factor-2 kinase-regulated pathway. *Am J Pathol*. 2010;177:481-492.
37. Fremont L. Biological effects of resveratrol. *Life Sci*. 2000;66:663-673.
38. Park DW, Baek K, Kim JR, et al. Resveratrol inhibits foam cell formation via NADPH oxidase 1-mediated reactive oxygen species and monocyte chemotactic protein-1. *Exp Mol Med*. 2009;41:171-179.
39. Yousuf S, Atif F, Ahmad M, et al. Resveratrol exerts its neuro-protective effect by modulating mitochondrial dysfunctions and associated cell death during cerebral ischemia. *Brain Res*. 2009;1250:242-253.
40. Sebai H, Gadacha W, Sani M, Aouani E, Ghanem-Boughanmi N, Ben-Attia M. Protective effect of resveratrol against lipopolysaccharide-induced oxidative stress in rat brain. *Brain Injury*. 2009;23:1089-1094.
41. King RE, Kent KD, Bomser JA. Resveratrol reduces oxidation and proliferation of human retinal pigment epithelial cells via extracellular signal-regulated kinase inhibition. *Chem-Biol Interactions*. 2005;151:143-149.